Performance modeling of an airborne Raman water vapor lidar

D. N. Whiteman, G. Schwemmer, T. Berkoff, H. Plotkin, L. Ramos-Izquierdo, G. Pappalardo

February 15, 2000

Abstract

A sophisticated Raman lidar numerical model has been developed. The model has been used to simulate the performance of two ground-based Raman water vapor lidar systems. After tuning the model using these ground-based measurements, the model is used to simulate the water vapor measurement capabilty of an airborne Raman lidar under both day- and night-time conditions for a wide range of water vapor conditions. The results indicate that, under many circumstances, the daytime measurements possess comparable resolution to an existing airborne differential absorption water vapor lidar while the nighttime measurements have higher resolution. In addition, a Raman

lidar is capable of measurements not possible using a differential absorption system.

1 Introduction

The Raman lidar technique has long been considered to be one of the finest techniques for ground-based monitoring of the nighttime evolution of atmospheric properties. Raman lidar studies which have been performed include the water vapor dynamics of frontal passages [10], aerosol growth and its relation to relative humidity [5], upper tropospheric and stratospheric temperature structure [4] and cloud droplet radius and number density retrievals [15].

Recently an automated Raman lidar [6] capable of daytime and nighttime measurements of water vapor and aerosols has been developed under the Department of Energy (DOE) Atmospheric Radiation Measurements (ARM) Program [12]. Despite the great success of Raman lidar technology from ground-based platforms, there has been very limited use of Raman lidars from aircraft. To date only nighttime, up-looking airborne Raman lidar measurements have been made [7] [3].

As a part of the National Aeronautics and Space Administration (NASA) Instrument Incubator Program, we have investigated the design and performance of an airborne Raman lidar which would be capable of a broad range of high priority scientific measurements for use in such aircraft as the NASA DC-8. These measurements include water vapor and aerosol scattering/extinction/depolarization (day and night) and cloud liquid water and rotational Raman temperature (night).

Perhaps the most important of these proposed measurements is that of water vapor. Because of this, we have chosen to focus on the anticipated water vapor measurement capability of an airborne Raman lidar by performing detailed numerical simulations. A numerical Raman lidar model was constructed and used to study the anticipated measurements of this new system for

water vapor conditions ranging from sub-tropical to arctic. These results demonstrate that a significant performance increase is realized by operating a Raman lidar looking downward from an aircraft compared to that same system looking upward from the ground. This improvement makes an airborne Raman lidar a very attractive airborne research tool for both daytime and nighttime conditions.

In the next section, the model will be described. This description includes a comparison of the model's calculation of the lidar overlap function [9] with ray tracing results. A sequential description of how the model is used to simulate lidar measurements is then given.

In section 3, the model is tuned to match the performance of two ground-based Raman lidar systems which use wide field of view and narrow field of view optical systems, respectively. Water vapor and nitrogen signals are simulated for each system. These simulated signals are then processed to yield a simulated profile of water vapor mixing ratio which is then compared to actual measurements.

The technical specifications for the airborne Raman lidar to be modeled are given in section 4. This lidar is based on a 0.6 m telescope. The performance of this system is studied for three different water vapor conditions ranging from sub-tropical to arctic.

In section 5, the candidate aircraft that have been surveyed are described. This aircraft survey indicates that for some measurement scenarios, the available viewport size is limited to 0.4 m. Simulations are performed of both down-looking and up-looking measurements using a 0.4 m telescope.

2 The model

A sophisticated Raman lidar model has been developed using the Mathematica programming language. The standard single scattering Raman lidar equation (equation 7.64 from reference [9]) has been used. In the evaluation of this equation, it is necessary to quantify the lidar system overlap function. The lidar overlap function describes the fraction of light that is transmitted through the lidar optical system as a function of range due to geometrical and optical effects. The overlap function results partly from the fact that the laser beam may not be fully in the field of view of the telescope for close ranges. The other major component of the overlap function results from the fact that objects at different distances in the telescope's object field are focussed at different points in the telescope's image field.

The model is used to simulate the measurement performance of an individual lidar detector channel. In the simulations done here, only water vapor and nitrogen Raman signals have been simulated although Rayleigh-Mie signals are also possible. The sequence of using the model to best simulate the measurement of an actual lidar system is as follows.

1) The lidar system overlap function is calculated using the following inputs: telescope primary diameter, telescope secondary diameter, telescope field of view, telescope F/number, telescope blur circle, laser divergence, initial laser beam diameter, and telescope focus range. In addition, a Gaussian laser beam profile can be specified. The shape of the Gaussian function can be adjusted to best fit the overlap behavior of the actual data. Only co-axial geometries are presently handled.

2) With the overlap function quantified, the single scattering lidar equation is evaluated as a function of range. This yields a simulation of the lidar system's measurement of water vapor or

nitrogen. The following input information is required: laser pulse energy, laser repetition rate, laser wavelength, Raman return wavelength, round trip attenuation due to molecular transmission and aerosol extinction, water vapor or nitrogen density profile (usually obtained from a coincident radiosonde launch), Raman scattering cross section, zenith angle, averaging time, data acquisition bin time, spectral width of the interference filter, filter transmission, photomultiplier tube quantum efficiency, photon counting bandwidth (if photon counting is to be simulated) and photomultiplier dark count rate (a value of 100 sec^{-1} was used for these simulations). All of these parameters are known for the system that is being simulated. Two more parameters are required as input to the model that are not necessarily known: irradiance of the background scene and the lidar channel optical efficiency (which accounts for the transmission efficiency of the optical components that have not already been specified such as collimating optics and beamsplitters). Reasonable values for these parameters are chosen at this point to generate an initial profile.

3) The simulated profile which results from step 2 is compared to the actual profile generated by the lidar. The model inputs for lidar channel optical efficiency and the background irradiance are then adjusted and another profile is generated. This process is repeated until the best match between the model output and real data is obtained. This process is referred to as "tuning" and results in values of background scene irradiance during the actual lidar measurement and the efficiency of the optical system.

2.1 Overlap function

As a demonstration of the model's ability to simulate lidar system overlap functions the following test case was studied using both the numerical Raman model and the commercially available opti-

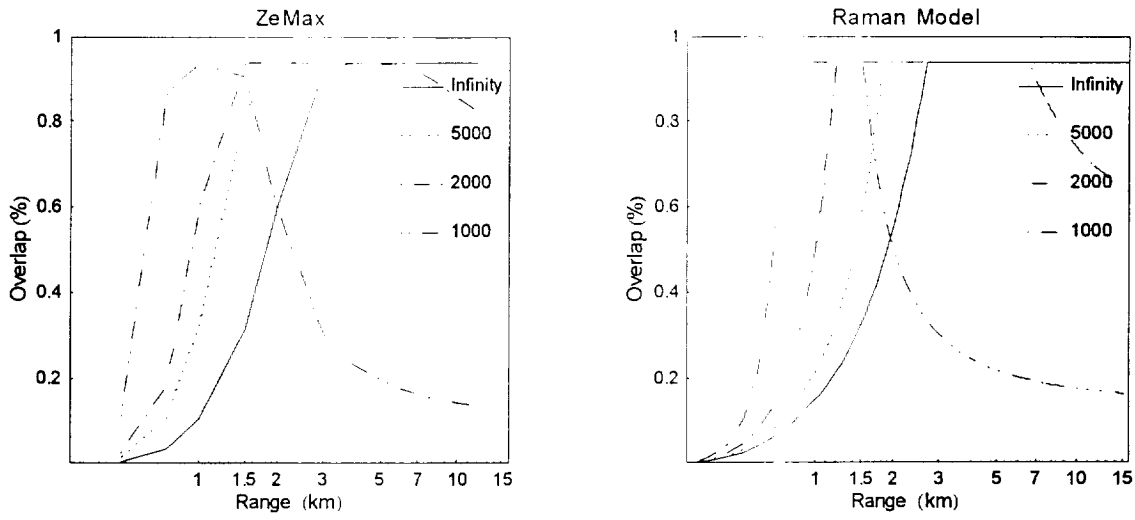

Figure 1: Comparison of the overlap function for a 0.6 m F/4 telescope using the ZeMax optical ray trace program and the Raman lidar model for diffrerent telescope focus settings: 1 km, 2 km, 5 km and infinity. The two sets of overlap functions show good qualitative agreement.

cal ray tracing program ZeMax. The lidar system that was modeled used an F/4, 0.6 m diameter telescope with a 0.15 m diameter secondary. For these simulations, an expanded laser beam of 100 mm diameter with divergence of 60 microradians. was used. The far field laser beam pattern was assumed to be uniform. A coaxial arrangement of the outgoing laser beam and the telescope optical axis was used. The results of this comparison for various telescope focus ranges are shown in figure 1 .

The two approaches for simulating lidar system overlap show good qualitative agreement. Since the model will be tuned to match actual ground-based lidar data before being used to simulate the performance of an airborne system, what one needs from a model is for it to give realistic behavior when a particular parameter is varied. The Raman model demonstrates very good ability to account

for variations in factors which influence the shape of the lidar system overlap function based on the results shown in figure 1.

Another factor that influences the shape of the lidar return signal when a photon counting detection system is used is photon pileup. Photon pileup is the term used to describe the probability that two photons may arrive closely spaced enough in time to not be individually distringuishable. In the model, this effect is simulated using a paralyzable assumption [13]. After the simulated profiles are created, the photon counting data are processed using a non-paralyzable assumption [13]. By using different mathematical expressions for photon pileup in these two stages of the modeling process, non-linearities are introduced into the processed data as the count rate increases. This simulates the difficulty of processing photon counting data that exhibit photon saturation effects.

3 Model tuning by comparison with ground-based data

3.1 Lidar systems to be modeled

The data from two different ground-based Raman lidar systems were used for model tuning and validation. Those systems are the NASA/Goddard Space Flight Center Scanning Raman Lidar (SRL) and the Department of Energy (DOE) Cloud and Radiation Testbed (CART) Raman Lidar. After tuning the model to accurately simulate these ground-based systems, airborne simulations under a wide range of water vapor conditions will be simulated.

3.1.1 Scanning Raman Lidar (SRL)

The NASA/GSFC Scanning Raman Lidar is housed in a single mobile trailer and contains two

lasers. For nighttime operations, a XeF excimer laser (351 nm) is used with output power of 12-24 W. For daytime measurements, a frequency-tripled Nd:YAG (355 nm) is used with output power of approximately 9 W.

Lidar measurements are made of the Rayleigh-Mie return at the laser wavelength as well as Raman shifted returns due to atmospheric water vapor, nitrogen and oxygen. When using the XeF excimer laser, the Raman shifted return wavelengths for water vapor, nitrogen and oxygen are approximately 403, 382 and 371 nm, respectively. The corresponding wavelengths for the Nd:YAG based measurements are approximately 408, 387 and 376 nm. All four of these signals are collected by a 0.76 m, F/5.2, variable field-of-view (0.25 - 2.5 milliradians) Dall-Kirkham telescope. The telescope is mounted horizontally and aligned with a large (1.2m x 0.8m) flat scan mirror. The scan mirror enables 180 degree scanning in a single scan plane.

The telescope output is collimated and then split among eight photomultiplier tubes (PMT) using dichroic beamsplitters and interference filters. There are two PMTs used to detect each wavelength. One PMT receives a small portion of the signal intensity and is used for the low altitude returns below approximately 4 km while the second PMT receives the remainder of the signal and is used for the high altitude returns above approximately 3 km. These PMTs are referred to as low and high channels, respectively. A more complete description of the SRL can be found in reference [15].

3.1.2 CART Raman Lidar (CARL)

The CART Raman Lidar was developed as a part of the DOE Atmospheric Radiation Measurements (ARM) Program and has been operational at the northern Oklahoma Cloud and Radiation

Testbed (CART) site since 1997. It uses a 0.6 m, F/9 telescope, 12 W Nd:YAG laser and is vertical pointing only. It is an automated system designed for 24-hour unattended operation. It makes all of its measurements using a narrow-band, narrow field of view detection technique. In addition to the measurements made by the SRL, it also measures aerosol depolarization. In a similar fashion to the SRL, CARL uses two photomultipliers for each wavelength. Thus, there is in general a high and low channel for each of the signals. Neutral density filters are used in the water vapor and nitrogen channels to decrease the count rates under some conditions in order to limit the effects of photon pileup correction [13]. The water vapor signal intensity is reduced by a factor of approximately 10 for daytime measurements while the nitrogen signal is reduced by a factor of approximately 20 under all conditions. A complete description of this system can be found in Goldsmith et. al. [6].

Only the high channel signals for both the SRL and CARL will be simulated here since, as will be shown, an airborne Raman lidar is capable of making measurements from 10 km to the surface with just a single channel.

3.2 Case study 1: Scanning Raman Lidar data (wide field of view)

The model will first be used to best simulate data acquired by the SRL during the third Convection and Moisture Experiment (CAMEX3) which occurred in August -September, 1998. The goal of CAMEX-3 was to better understand the genesis and tracking of hurricanes by acquiring a comprehensive set of measurements of both the hurricane developmental environment and the hurricane itself. Measurements were acquired both from airborne and ground-based platforms as a part of this field experiment.

The SRL was situated on Andros Island in the Bahamas as a part of the calibration/validation fa-

cility for the CAMEX-3 campaign. In addition to the SRL, this ground site included the University of Wisconsin Advanced Emitted Radiance Interferometer (AERI), radiosonde launch systems provided by both NASA/GSFC Wallops Flight Facility and the University of Wisconsin, Global Positioning System measurements of column water vapor, sun photometer measurements of aerosols and water vapor and standard surface sensor measurements of temperature, pressure and relative humidity [16].

During the course of the nearly two-month deployment on Andros Island, the water vapor and aerosol environment associated with the nearby passage of hurricanes Bonnie, Danielle, Earl and Georges was measured. On the night of August 22, 1998 during the passage of hurricane Bonnie, one of the several calibration/validation overflights of Andros Island by the NASA DC-8 aircraft occurred. On board the DC-8 for this experiment was the NASA/Langley Research Center (LaRC) differential absorption LASE (Lidar Atmospheric Sensing Experiment) water vapor lidar system. This overflight provided an opportunity to compare the ground based water vapor measurements of the SRL with those of the airborne LASE.

LASE [2] is a differential absorption lidar based on a tunable Ti:sapphire laser operating at 5 Hz with output wavelength in the 815 nm region of the spectrum. Pulse output energy is 100mj. During the Andros overflights, LASE was operated in simultaneous up-looking and down-looking modes so that approximately 70% of the laser energy was directed downward. In addition, in order to measure the complete range of water vapor present from the upper troposphere to the surface, three water vapor absorption line pairs of varying absorption strength were cycled among during flight. Thus, 6 separate laser pulses were required to cover all 3 line pairs.

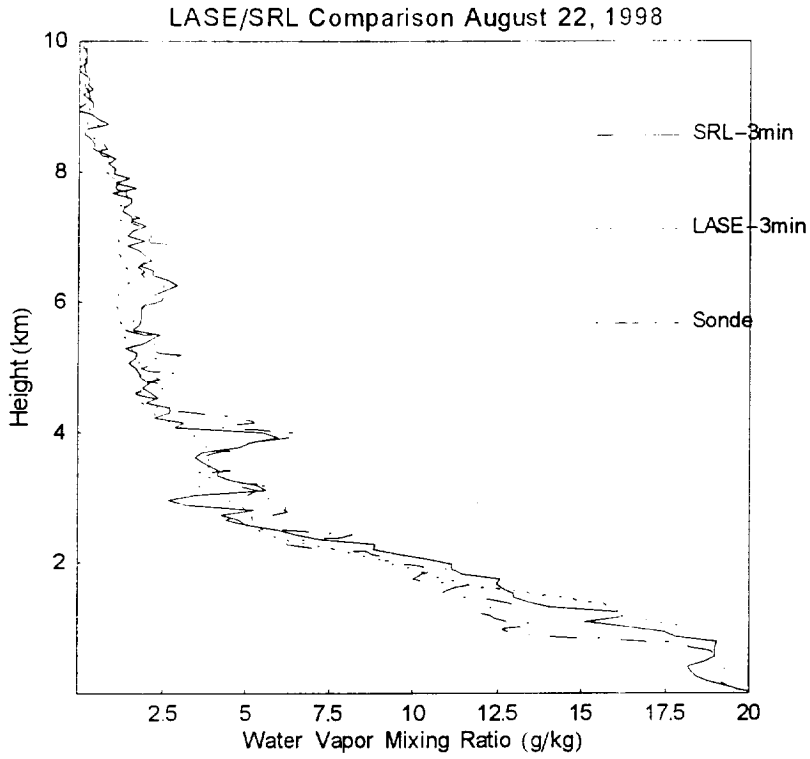

Figure 2: Comparison of water vapor mixing ratio measurements of the airborne LASE differential absorption lidar and the ground-based SRL. Also shown is a radiosonde launched at 0022 UTC which was approximately 30 minutes before the aircraft overflight. Both the LASE and the SRL profiles use 3 minute averages.

The comparison of SRL and LASE water vapor measurements made during this overflight is shown in figure 2. Also shown is a Vaisala RS-80H radiosonde measurement of water vapor which occurred at 0022 UTC. The radiosonde launch occurred approximately 30 minutes prior to the DC-8 overflight.

The three datasets show good general agreement except in the regions between 1-2 km and between 5-8 km. Between 1-2 km the SRL and LASE indicate higher moisture levels than the

radiosonde. Between 5-8 km, the SRL and radiosonde agree well while LASE shows lower moisture. Several factors must be considered in the comparison of these datasets, however. First, it should be noted that a cloud was present at approximately 1 km during a portion of the 3 minute LASE averaging period. This prevented LASE water vapor retrievals lower than 1 km. In addition, during the three minute averaging period of the LASE data, the DC-8 travels approximately 30-40 km. This can result in both smoothing of features in the water vapor profile as well as changes in those features. Finally, the vertical resolution of the instruments is very different. The resolution of the LASE data is 330 meters between 0-2 km, 510 meters between 2-6 km, and 990 meters between 6-8 km. The SRL data have 75 meter vertical resolution throughout the profile and the radiosonde data are reported at 50 meter resolution throughout the profile.

3.2.1 Water vapor signal tuning

The water vapor mixing ratio is calculated from the ratio of the Raman signals for water vapor and nitrogen [13]. The model must therefore be able to accurately simulate lidar signals for these molecular returns. The raw SRL water vapor and nitrogen data from the same overflight period shown in figure 2 were used to tune the model to simulate SRL performance. These SRL data were acquired using a 2 milliradian field of view on the SRL telescope. The model was first used to calculate the overlap function using SRL system parameters. Then the model was used to simulate high channel SRL water vapor and nitrogen signals using input profiles for both the water vapor mixing ratio and the atmospheric density from the 0022 UTC radiosonde. (Using the radiosonde data as input to the model instead of the lidar-derived water vapor mixing ratio allows differences induced by random error to be more easily discerned since the radiosonde has similar

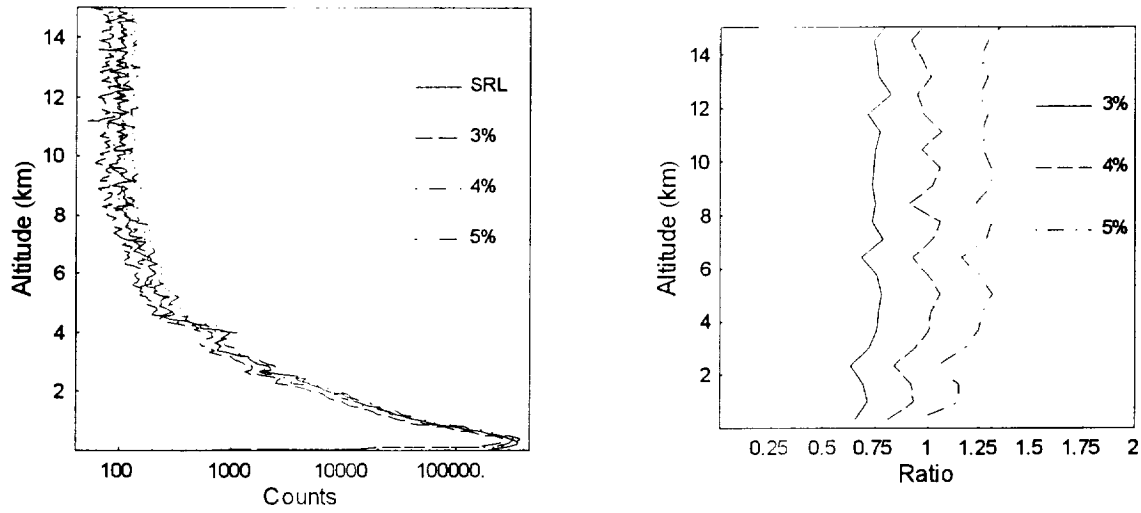

Figure 3: Illustration of model tuning for the optical efficiency parameter. On the left is plotted the simulated SRL water vapor signal for a range of optical efficiencies. On the right is plotted the ratio of the model output to the SRL data (smoothed to 400m resolution for easier interpretation). Notice that the curves are separated throughout the profile. The value of 4% gives the best agreement between the data and the model.

noise characteristics through most of the troposphere while the noise in the lidar signal increases with height.)

The process of tuning the model to predict SRL performance involves entering all the known SRL parameters into the model and then varying the lidar system optical efficiency and sky background radiance so that the model output matches the actual profile. Tuning the model for optical efficiency is illustrated in figure 3 using the SRL high channel water vapor profile.

The influence of changing the water vapor channel optical efficiency parameter is shown in figure 3. The values of 3%, 4% and 5% were used to quantify the efficiency of the receiver optics

excluding the interference filter and the PMT quantum efficiency which were separately quantified as 50% and 23%, respectively. In the left hand plot, the actual SRL water vapor signal is plotted along with the three simulated signals all using 1-minute averages. Random error in the model is simulated assuming Poisson statistics. The value of 4% most closely matches the actual SRL data as can be seen in the plot on the right which shows the ratio of simulated and actual data. The influences of the lidar system overlap function and photon counting saturation can be seen in this ratio below an altitude of approximately 1 km. The curves in the plot on the right show a relatively constant separation with altitude since the optical efficiency influences all parts of the profile similarly.

Model tuning for the background radiance is shown in figure 4. The values of 0.2, 0.25, 0.3 x 10^{-7} $W\ cm^{-2}\ sr^{-1}\mu m^{-1}$ were used for background radiance. For all model profiles shown in this figure, the lidar system efficiency used was 4%. In the lowest part of the profile, the curves overlay each other almost exactly. This is due to the fact that at high signal strengths such as exist for near range returns, the lidar signal is much larger than the nighttime sky background. At higher altitudes, however, the curves are seen to separate as the influence of background light becomes larger. The value of 0.25 x 10^{-7} $W\ cm^{-2}\ sr^{-1}\mu m^{-1}$ was chosen to best represent the background radiance for this SRL profile.

3.2.2 Nitrogen signal

In a manner similar to the tuning just shown for water vapor, the model was tuned to simulate the high SRL nitrogen channel optical efficiency. During this process, the background radiance was kept the same as for the water vapor channel. Figure 5 shows the comparison of SRL high channel

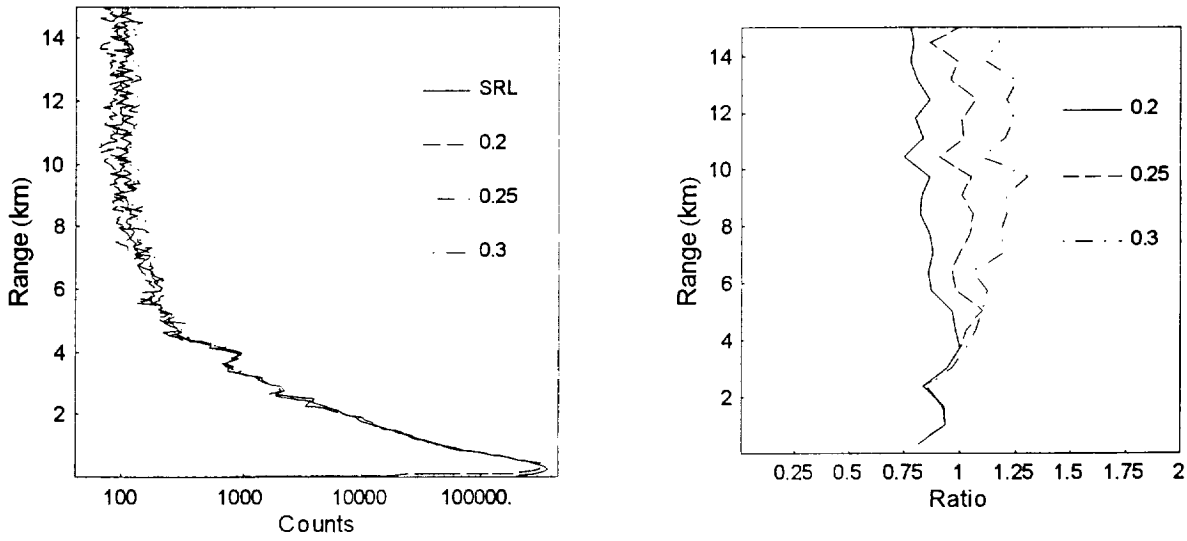

Figure 4: On the left is shown the result of using a 4% optical efficiency and changing the value of background radiance in units of 10^{-7} W cm^{-2} sr^{-1} μm^{-1}. Here all curves converge in the lowest part of the profile where the background light level has essentially no influence. The ratio of the model to SRL has been smoothed to 400m for easier interpretation. The values of 0.25 x 10^{-7}gives the best agreement between the data and the model.

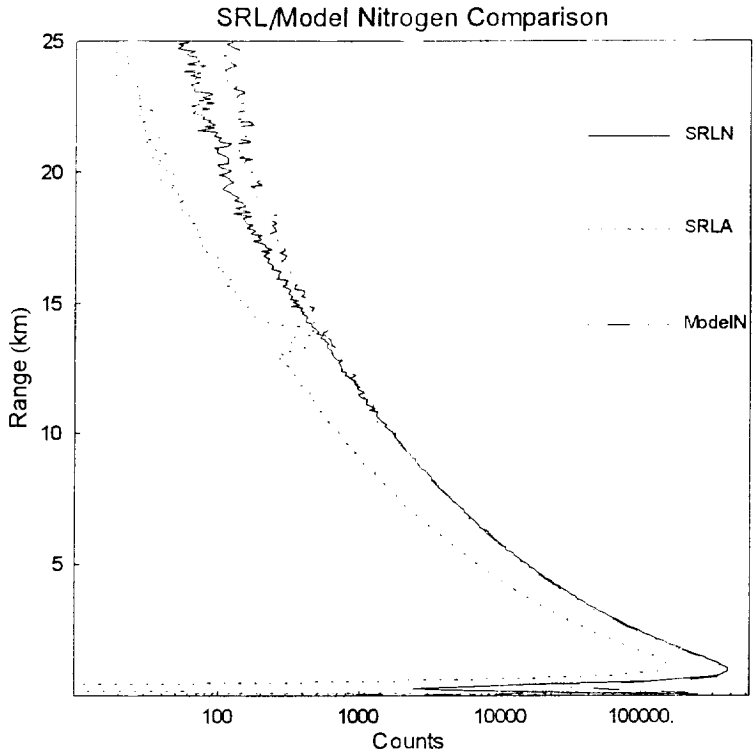

Figure 5: Comparison of actual 1 minute SRL nitrogen channel data and the output of the Raman model. The two curves agree very well up to an altitude of about 13 km where the SRL aerosol channel shows the presence of a cirrus cloud that was not accounted for in the model.

nitrogen and aerosol data. All profiles use a 1 minute average.

The model and the SRL high channel nitrogen data (SRLN) agree very well up to an altitude of about 13 km. At this point the two curves diverge. The simultaneously acquired SRL aerosol data (SRLA) are plotted to show the presence of a cirrus cloud between 13-14 km. The actual SRL nitrogen data show the influence of the additional extinction due to this cirrus cloud. The model was not told of the presence of the cirrus cloud, however. The amount of separation of the model and the SRLN curves above the height of the cirrus cloud can be used to quantify the optical depth

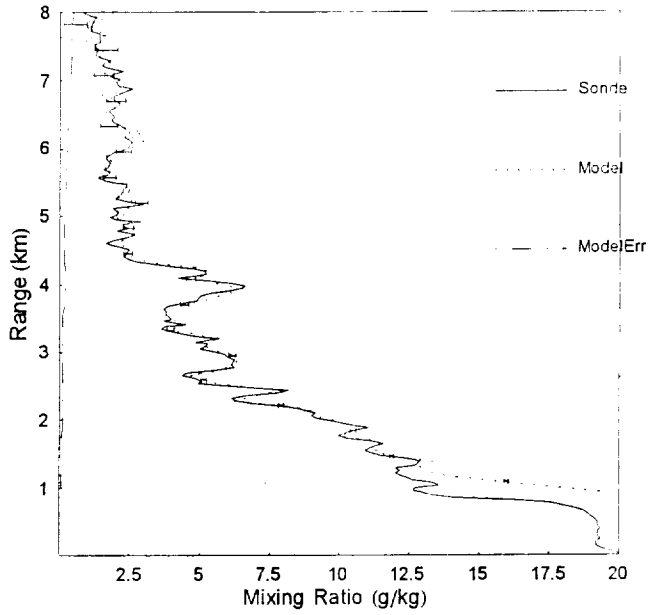

Figure 6: Comparison of radiosonde water vapor profile and 1 minute water vapor mixing ratio as predicted by the model. The model used 1 minute averaging and 75m vertical resolution.

of the cloud.

3.2.3 Model water vapor mixing ratio

Now that the simulated water vapor and nitrogen high channel signals are available, these simulated data can be processed for water vapor mixing ratio in the same way as real data. These results are shown in figure 6.

The agreement between the model and the radiosonde is excellent above 2 km indicating that the model has accurately reproduced the lidar signals corresponding to the high channel measurement of water vapor mixing ratio. Below 2 km, the curves disagree because the high channel lidar

signals are influenced by photon counting saturation in this part of the profile illustrating the need for low channel detectors for ground based, photon counting measurements. The standard error in the simulated water vapor mixing ratio as determined by Poisson statistics is also shown.

3.3 Case study 2: DOE/CART Raman lidar data (narrow field of view)

One of the techniques used for Raman lidar measurements in the daytime employs a narrow field of view telescope and narrow bandpass filters. Both of these decrease the amount of background light that gets to the detectors which allows the weak Raman signals to be measured even under bright daytime conditions. The CART Raman lidar (CARL) uses this approach by operating with a field of view of approximately 0.25 milliradians and by using interference filters which are approximately 0.4 nm wide. To validate the model's ability to simulate narrow field of view measurements, data acquired by CARL on the night of September 27, 1997 were used. The model was given a 10-minute average water vapor mixing ratio profile from the lidar (using both high and low channels) as input along with number density from a radiosonde launched at the site on that evening. Figure 7 shows the comparison of the model simulations of a 1-minute average of water vapor and nitrogen data and the actual 1-minute water vapor and nitrogen data acquired by the CARL high channels. The model agrees very well with the actual data even in the lowest portions of the profile where the influence of the narrow telescope field of view is largest.

These simulated signals were then processed to yield water vapor mixing ratio. The fully processed 1-minute model simulation of water vapor mixing ratio is shown in figure 8 along with the actual 10-minute CARL measurement. The agreement is excellent above 3 km. Again, only the high channels have been simulated here so that the disagreement below 3 km is due to photon

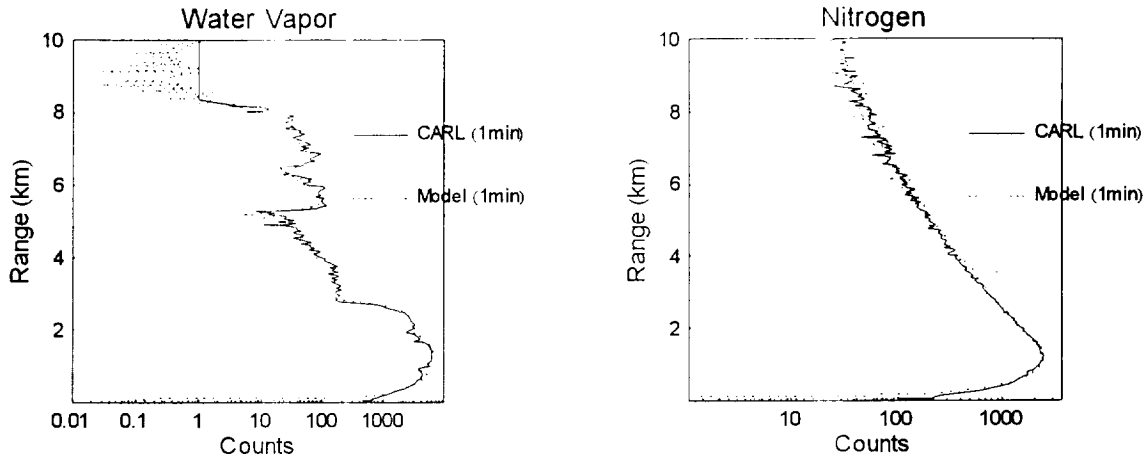

Figure 7: Comparison of DOE/CART Raman lidar (CARL) high channel water vapor and nitrogen signals and model simulations. CARL uses a narrow field of view detection technique to enhance daytime measurements. The model is able to accurately simulate CARL narrow field performance.

count saturation.

3.3.1 Model tuning for daytime conditions

The model was next used to simulate the daytime performance of the CART Raman lidar. Figure 9 shows the results of the model tuning for daytime measurements acquired by CARL on September 27, 1997 at 1500 UT. Again the agreement between the model and actual data is very good. The background radiance required by the model to match the CARL data was 1.1 x 10^{-2} $W\ cm^{-2}sr^{-1}\ \mu m^{-1}$. Modtran calculations using rural aerosol loading, standard atmospheric density and the known solar zenith angle of 60 degrees indicated a radiance of approximately 1.0 x $10^{-2}\ W\ cm^{-2}sr^{-1}\ \mu m^{-1}$ in good agreement with the model.

As an additional test of the model's treatment of background radiances, CARL data acquired

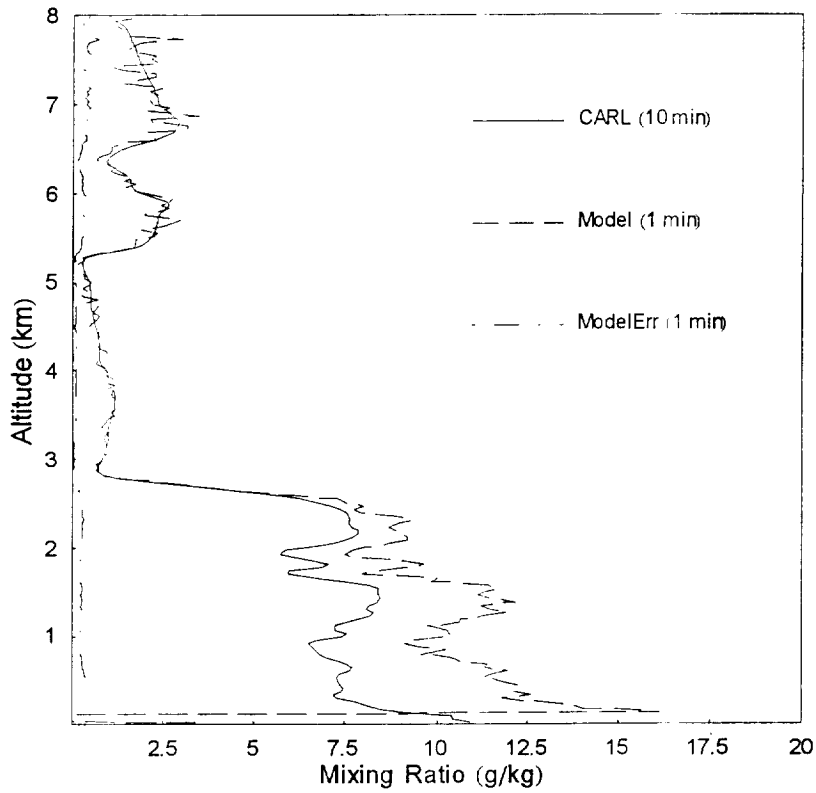

Figure 8: Comparison of a 10-minute nighttime water vapor mixing ratio measurement by the DOE CART Raman lidar and model predictions of the CART system for a 1-minute measurement period. The agreement is excellent above 3 km. Below 3 km, the model simulation is influenced by the lidar overlap function and photon count saturation.

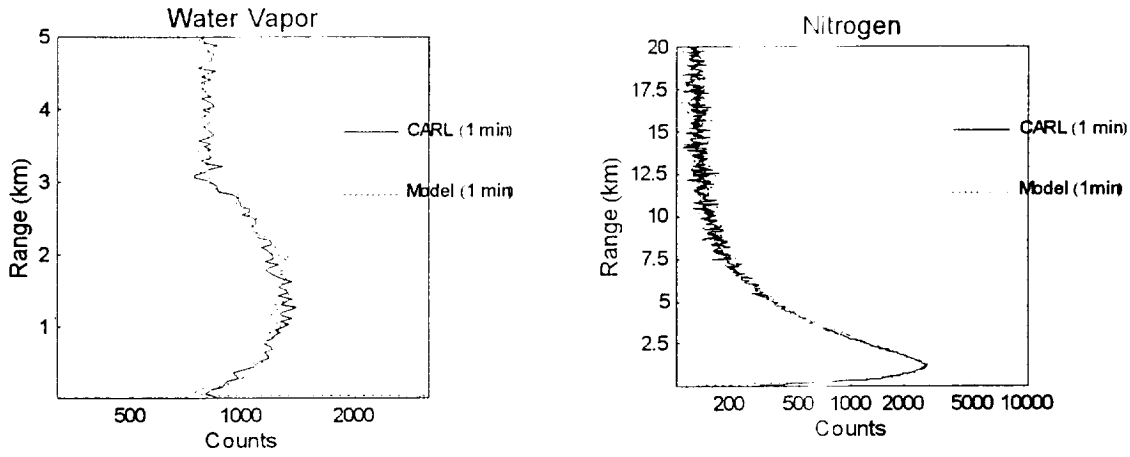

Figure 9: Comparison of model output and actual CARL measurements during the daytime on September 27, 1997. The solar zenith was 60 degrees.

with the highest sun angle on this day (38 degrees) were also simulated. For these data, the Raman model required a value of 1.5 x 10^{-2} $W\ cm^{-2}sr^{-1}\ \mu m^{-1}$ to match the actual lidar data. Modtran predicted a radiance level of approximately 1.7 x 10^{-2} $W\ cm^{-2}sr^{-1}\ \mu m^{-1}$ for this case. These two examples indicate that the model is accurately assimilating real sky radiances.

Using the same atmospheric conditions as in figure 9, a 10-minute simulation of water vapor mixing ratio was generated and compared with actual measurements. This is shown in figure 10. The CARL water vapor mixing ratio profile shown in the figure was used as input to the model for these simulations. The agreement is very good above 2.5 km where the high channels are used. Note that the error is plotted multiplied by 10 for easier viewing.

4 Airborne Simulations

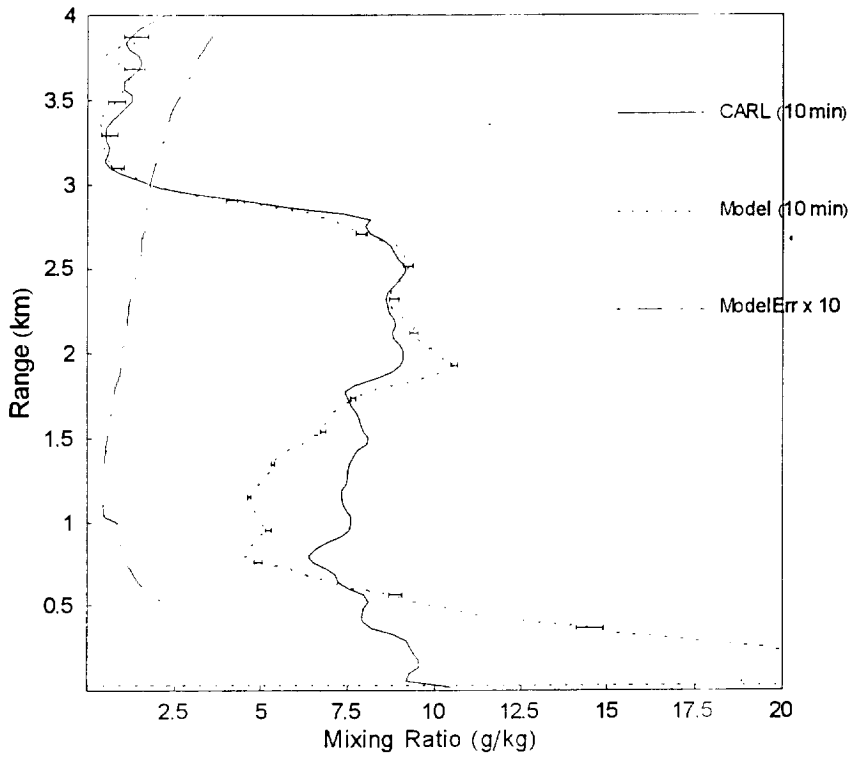

Figure 10: Comparison of daytime water vapor mixing ratio derived from simulated signals generated by the model and the actual CARL measurements made at 1500 UTC on September 27, 1997. Only the high data channels have been simulated so the curves agree well only above 2.5 km.

4.1 Lamont, Oklahoma - September 27, 1997

4.1.1 nighttime conditions

The model has been used to accurately simulate water vapor measurements of two ground-based Raman lidar systems. At this point, the model will be used to simulate the performance of a Raman lidar system from an airborne platform. The parameters for the airborne system are shown in table 1. These parameters are the same as for the ground-based CARL lidar except for two modifications: the neutral density filters have been removed from the water vapor and nitrogen channels and the laser power has been increased to 15W. Due to the signal compression that occurs when measuring downward from an airborne platform, the dynamic range of the signal is greatly reduced and these neutral density filters are not needed as will be demonstrated later. The parameters of the modeled system are shown in Table 1.

Using the same input parameters as in the simulation shown in figure 8, water vapor and nitrogen signals were modeled for the airborne lidar and are shown in figure 11. A 15-second average was used. The signals have been converted to count rate. Several points can be made here. The advantages of measuring downward toward the surface using lidar is clear. All lidar systems are influenced by the inverse range squared decrease in the signal intensity with range. The advantage of making measurements downward from an airborne platform is that most species of interest (e.g. water vapor, nitrogen and aerosols) have higher concentrations nearer to the surface. This results in a compression of the dynamic range of the signal which has many advantages.

The lower 8 km of the airborne water vapor and nitrogen signals are both contained within

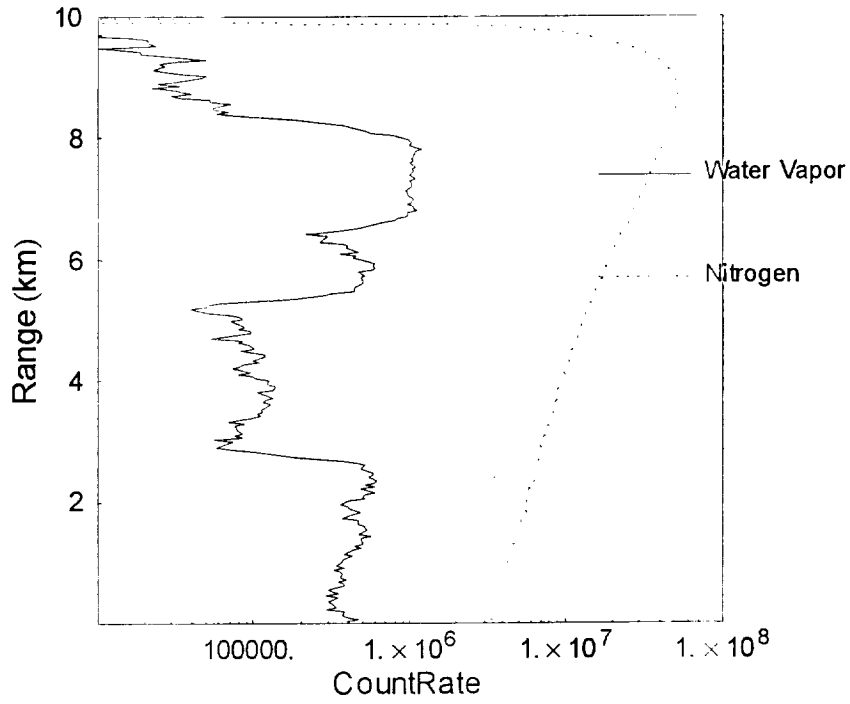

Figure 11: Model water vapor and nitrogen signals for the described airborne Raman lidar at a flight altitude of 10 km. The data have been converted to count rate (Hz). Both water vapor and nitrogen signals show significant dynamic range compression when compared with figure 7.

approximately 1 decade of dynamic range. This is compared with the nearly 4 decades (2 decades) of dynamic range required to make the water vapor (nitrogen) measurement from the ground as was shown in figure 7. Because of this dynamic range compression for an airborne lidar, it is possible to measure the entire range of the lidar signal shown using a single detector. In addition, one would expect much better detector linearity and less susceptibility to such effects as signal induced noise when operating from the air due to this compression. Also, since the maximum count rates observed are approximately 50 Mhz, it would not be necessary to use any additional neutral density filtering to make these measurement from the air (a combination of photon counting and analog detection would be useful for a 50 Mhz signal to avoid the pulse pileup correction). These simulated signals have been analyzed for water vapor mixing ratio. The results are plotted in figure 12.

Along with the 15-second averaging time, vertical smoothing of 200 meters between 0 - 6 km, 120 m between 6 - 8 km and 40 m between 8 - 10 km has been used in the model. The random error in the model is shown multiplied by a factor of 10 for easier viewing. The random error is approximately 10% in the dry region between 3-5 km but drops to between 5-7% in the region near the surface. This figure illustrates an additional important advantage of operating a Raman lidar from the air. Due to the increase in signal strength at the farthest range in the profile, high quality measurements of water vapor mixing ratio are possible in a fraction of the time required by the same ground based system.

4.1.2 daytime conditions

Since there was good agreement between the background radiances required as input to the Raman

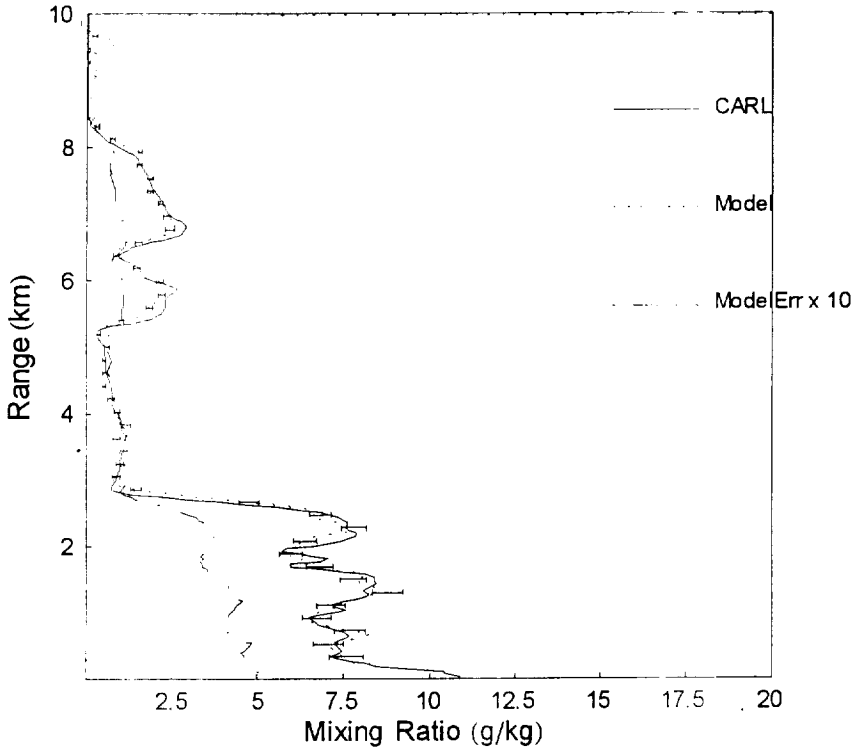

Figure 12: Simulation of the airborne Raman lidar at a flight altitude of 10 km. A 15 second averaging time is used. The profile has been smoothed as follows: 0 - 6 km: 200m, 6 - 8 km: 120m, 8 - 10 km: 40m. The model error is plotted multiplied by 10 for easier viewing. The random error is approximately 5-7% near the surface.

model in order to match actual upward-looking lidar data and those predicted by Modtran, Modtran was again used to predict the background radiance expected under a range of downward-looking conditions. Figure 13 shows the results of these Modtran runs.

Ocean, grass and fresh snow surfaces were simulated. The radiance is calculated for a range of solar zenith angles ranging from 0-75 degrees. As mentioned before, the value of radiance required to match the up-looking daytime CARL data acquired with a solar zenith angle of 38 degrees was 1.5 x 10^{-2} $W\ cm^{-2}sr^{-1}\ \mu m^{-1}$. Under these conditions the Modtran prediction was 1.7 x 10^{-2} $W\ cm^{-2}sr^{-1}\ \mu m^{-1}$. Figure 13 illustrates that these upward-looking radiance values are equal to or larger than the largest down-looking radiances for any solar zenith angle over either an ocean or grass surface. This demonstrates another advantage of operating a Raman lidar from an aircraft versus the ground. Under many conditions, the background radiance levels are lower looking downward than they are looking upward making it easier to measure the weak Raman signals under daytime conditions.

To simulate the performance of the airborne Raman lidar under daytime conditions at the DOE CART site a value of background radiance of 1.3 x 10^{-2} $W\ cm^{-2}sr^{-1}\ \mu m^{-1}$ was used. This value is consistent with a grass surface and a solar zenith angle of approximately 30 degrees. All other parameters were the same as for the nighttime retrievals shown in figure 12 except that the averaging time was increased to 3 minutes. The results are shown in figure 14.

The figure shows the comparison between the 10-minute ground-based CARL measurement (nighttime profile) and the simulated airborne Raman measurements for the water vapor conditions of September 27, 1997 at the northern Oklahoma CART site. A three minute averaging time has

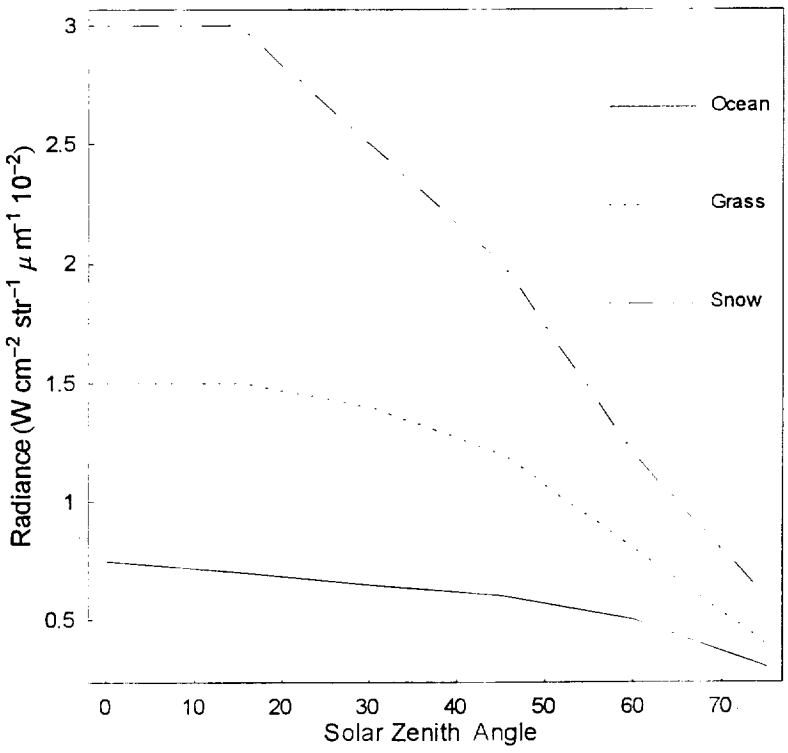

Figure 13: Radiances looking downward from 10 km for a range of solar zenith angles and for three surfaces: ocean, grass and fresh snow. The value of radiance required to match the uplooking daytime measurements ($1.5 \times 10^{-2}\ W\ cm^{-2} sr^{-1}\ \mu m^{-1}$) is as large or larger than any downlooking radiance over ocean or grass surfaces.

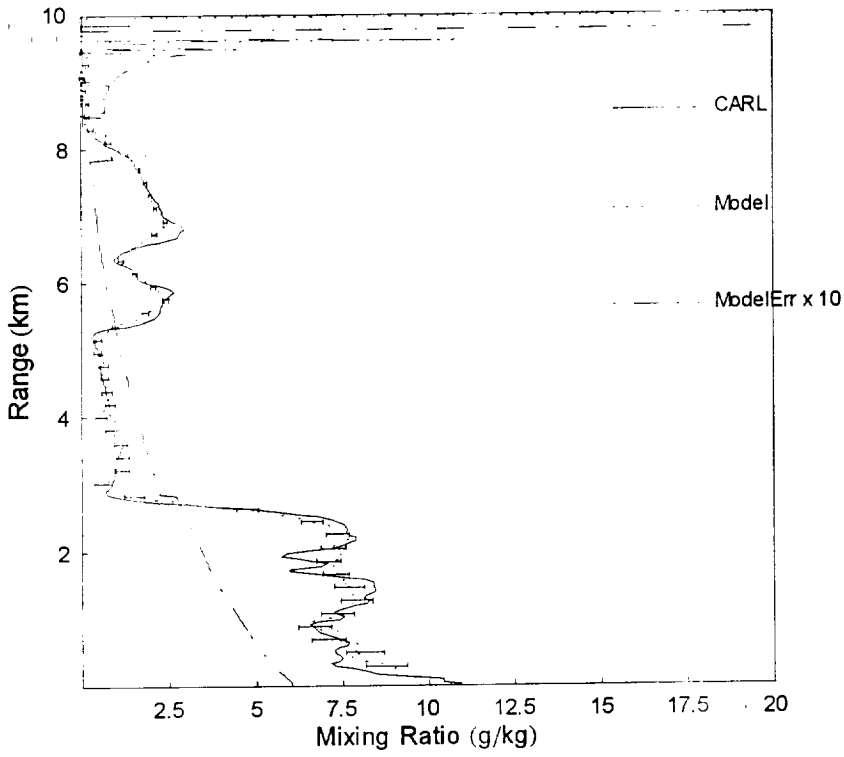

Figure 14: Simulated airborne retrievals from a flight altitude of 10 km for daytime conditions. The background radiance used was for 38 degree solar zenith angle over a grass surface which simulates the measurement conditions at the time of highest sun angle on September 27, 1997 in northern Oklahoma.

been used in the model and the profile has been smoothed to 350 meters between 0-3 km, 520 meters between 3-8 km and 40 meters between 8-10 km. The random error near the surface is between 5-7% as in the nighttime case, however the random error in the dry region between 3-5 km, where the mixing ratio values range between 0.3 - 1.2 g/kg, has increased to approximately 20%.

4.2 Andros Island, Bahamas - August 22, 1998

4.2.1 nighttime

The performance of the airborne Raman lidar can now be assessed for the same measurement conditions under which the measurements in figure 2 were made. Figure 15 shows the simulated performance of the airborne Raman lidar under the nighttime conditions that existed during these measurements.

The airborne Raman lidar simulation is for a measurement time of 10 seconds and uses vertical smoothing as follows: 0 - 4 km : 200 meters, 4 - 7 km: 120 meters, 7-10 km : 40 meters. The random error in the retrieval is less than 10% up to 9 km and closer to 5% in the very moist region near the surface.

4.2.2 daytime

In order to simulate daytime measurement conditions in the Bahamas, the background radiance chosen was that for a 0 degree solar zenith angle over the ocean. The Modtran radiance for these conditions when down-looking from 10 km was $0.75 \times 10^{-2}\ W\ cm^{-2} sr^{-1}\ \mu m^{-1}$. All other param-

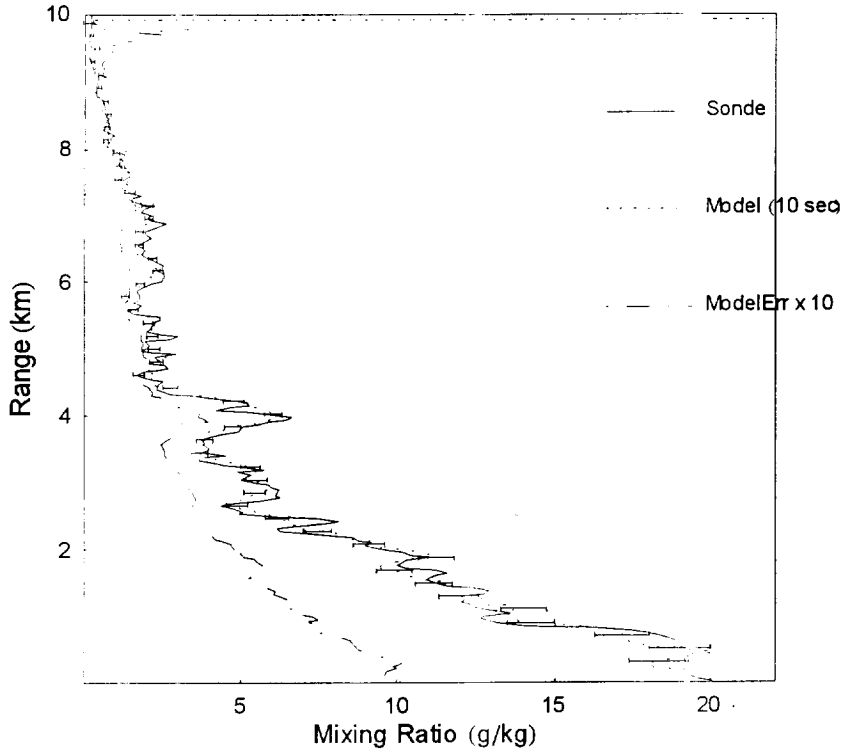

Figure 15: Simulated measurements of the airborne Raman lidar using the same atmospheric conditions as those shown in figure 2(Andros Island, Bahamas). The averaging time is 10 seconds and the vertical resolution is as follows: 0-4 km : 200 meters, 4-7 km : 120 meters, 7 - 10 km : 40 meters.

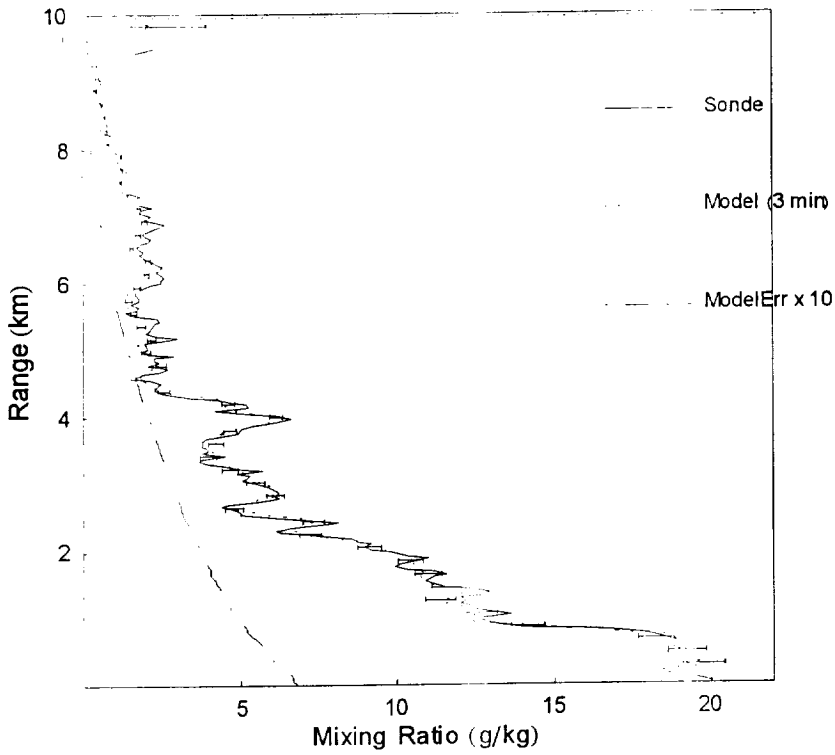

Figure 16: Simulated airborne Raman lidar measurements from an altitude of 10 km with background radiance equivalent to a 0 degree solar zenith angle over an ocean surface. The averaging time used was 3 minutes and the vertical smoothing is 0-9 km : 200 meters and 40 meters above.

eters were kept the same as in figure 15 except that the averaging time was increased to 3 minutes. The results are shown in figure 16.

The modeled Raman water vapor mixing ratio profile was smoothed to 200 meter vertical resolution between the surface and 9 km. The modeled error is generally less than 5% except in the region between 5 -6 km where it is closer to 7%. In the lowest 2 km of the profile, the error is 3-4%.

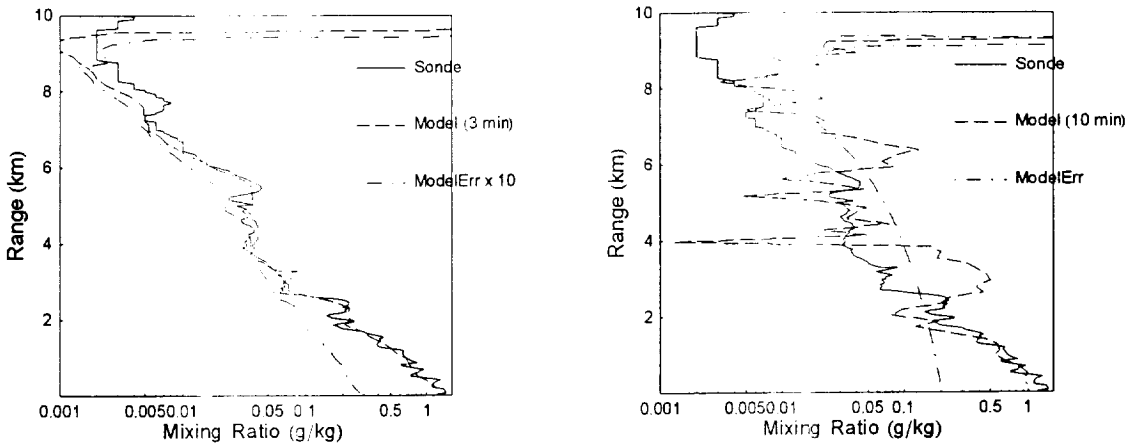

Figure 17: Modeled performance of the airborne Raman lidar system for simulated arctic conditions. Nighttime measurement performance using a 3 minute average is shown on the left and daytime performance using a 10 minute average is on the right.

4.3 Arctic conditions

To investigate the performance of this airborne Raman lidar over the widest range of conditions, arctic water vapor concentrations were simulated by using the upper portion of the August 22, 1998 Andros Island radiosonde. The model used the radiosonde water vapor values above 8 km as representative of an arctic profile beginning at the surface. The values in this simulated profile range from approximately 1.0 g/kg at the surface to values of 0.002 - 0.004 g/kg between 8 and 10 km. These values agree well with values reported recently (December, 1999) from the SOLVE (SAGE-III Ozone Loss and Validation Experiment) airborne measurement campaign held in Northern Sweden (Dr. Richard Ferrare, personal communication, January, 2000). The simulated nighttime and daytime performance is shown in figure 17.

The nighttime simulation used a 3 minute average and vertical smoothing of 450 m from the surface to 5 km and 750 meters above 5 km. Random error throughout the profile is less than 10% with the error near the surface being approximately 3%. For the daytime simulation, a 10 minute average has been used and the background radiance was that for a snow surface at a 40 degree solar zenith angle. The profile was smoothed to 1.05 km throughout the profile. Under these conditions the errors exceed 100% for all altitudes above 3 km. However, at the surface the error is less than 20%.

5 Aircraft Survey

Several aircraft have been investigated as possible platforms for testing an airborne Raman lidar of the specifications modeled here. Those aircraft are the NASA DC-8, P3 and C130 and a Northrup-Grumman 737. Both the NASA DC-8 stationed at Dryden Research Facility and the Northrup-Grumman 737 stationed at Baltimore Washington International airport are able to carry research payloads to altitudes of 10 km. The DC-8 has two viewports which measure 0.76 x 0.94 m. These are much more than adequate to accommodate the 0.6 m aperture of the modeled system. However, these viewports are located in the fore and aft cargo compartments where thermal variations can be expected during flight. Viewports as large as 0.4 m exist in the thermally controlled portion of the aircraft.

The Northrup-Grumman 737 has a window that measures 0.51 x 0.61 m and can thus accommodate most of the clear aperture of the modeled system. This window is in a thermally controlled part of the aircraft.

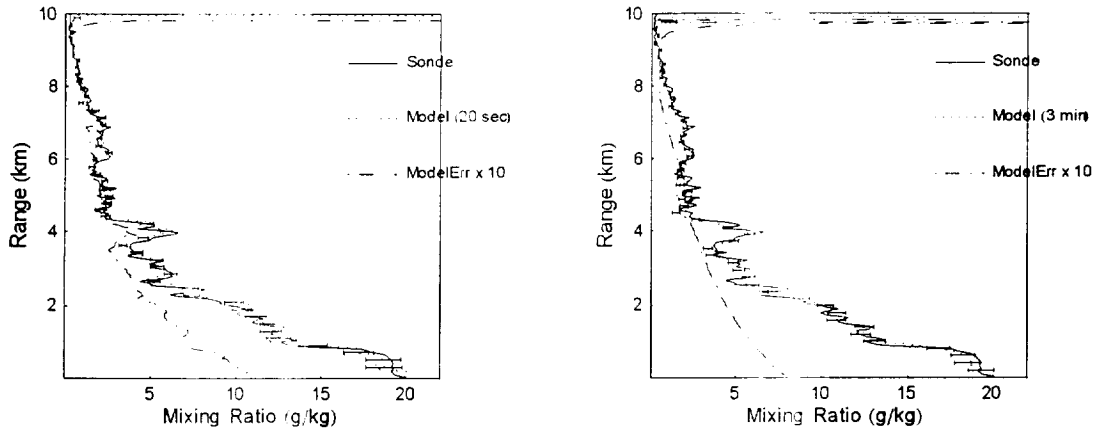

Figure 18: Model comparisons of a down-looking airborne Raman lidar using a 0.4 m telescope for the Andros Island case. The nighttime simulation uses a 20 second average while the daytime simulation uses a 3 minute average.

The P3 and C130 both have available apertures to accommodate the modeled telescope. The maximum flight altitude of these aircraft is approximately 8 km., however. All aircraft can provide sufficient power for the airborne Raman lidar system modeled.

5.1 Simulations using a 0.4 m telescope

In the passenger cabin of the DC-8, both down-looking and up-looking viewports with 0.4 m aperture are available. To investigate the possibility of flying in this part of the DC-8, simulations were done using a 0.4 m telescope for the modeled system with all other parameters remaining the same. The model results for the case of the August 22, 1998 conditions at Andros Island are shown in figure 18 for both nighttime and daytime conditions.

The nighttime simulation on the left uses an averaging time of 20 seconds with vertical smooth-

ing as follows: 0-6km: 200m, 6-8 km: 120m, 8-10km: 40m. The random error is again below 10% for the entire profile with values in the range of 5% near the surface. For the daytime simulation on the right, a 3 minute average has been used. The profile has been smoothed as follows: 0-5 km: 360m, 5-7 km: 200 m, 7-10 km : 40 m. Again the profile shows very good error statistics with error values everywhere below 10% and below 5% near the surface.

5.2 Upward looking simulations

An upward looking viewport accommodating a 0.4 m aperture telescope is available on the DC-8 aircraft. Therefore, it is interesting to simulate the nighttime performance of a 0.4m telescope based system for up-looking measurements from 10 km. To do this, the August 22, 1998 radiosonde water vapor profile from Andros Island, Bahamas was used as an input to the model. The same background radiance ($0.25 \times 10^{-7}\ W\ cm^{-2} sr^{-1}\ \mu m^{-1}$) used for the ground-based case shown in figure 6 was used here as well although it is reasonable to expect that the nighttime sky radiances would be lower looking upward from 10 km. The model used a field of view of 0.5 milliradians to decrease the influence of the overlap function. The results are shown in figure 19.

In these simulations, a 10-minute average has been used and the final water vapor profile has been smoothed to 1.05 km. The influence of the overlap function on the model simulations is evident up to an altitude of approximately 11.5 km. However, above this altitude, the agreement is very good. Also, despite the very small water vapor concentrations, the random error of the measurement is below 10% up to an altitude of 14 km where the water vapor mixing ratio is approximately 0.01 g/kg.

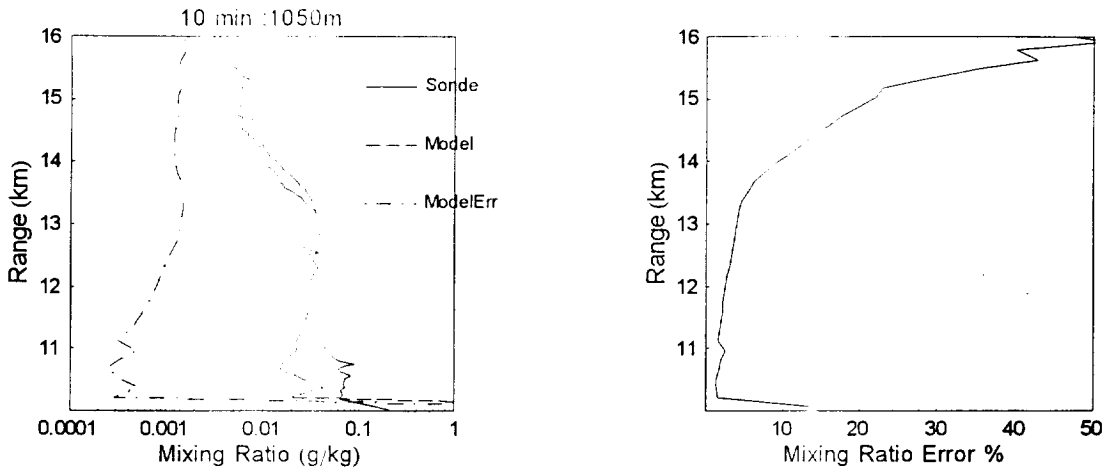

Figure 19: Simulation of the water vapor measurement performance of a 0.4 m aperture Raman lidar system looking upward from a 10 km flight altitude. A 10 minute average has been used along with 1.05 km vertical smoothing.

6 Summary and Discussion

The NASA/GSFC Raman lidar group has been funded through the NASA Instrument Incubator Program to construct an airborne Raman lidar. A Raman lidar numerical model has been constructed as a part of this effort. Model predictions have been tuned to best simulate the water vapor measurements of two ground-based lidar systems using both nighttime and daytime data. These comparisons show very good agreement. The sky radiances derived in this process agree well with Modtran. After tuning the model with ground-based data, measurement simulations of a candidate airborne Raman lidar system were performed for both daytime and nighttime conditions for several test cases covering a wide range of water vapor concentrations.

The cases studied include downward looking measurements from a 10-km flight altitude during

both the nighttime and the daytime for three sets of conditions: 1) September, 1997 at the DOE CART site in northern Oklahoma, 2) August, 1998 at Andros Island, Bahamas, and 3) simulated arctic conditions during December. For the first two cases, the simulations presented here indicate that the airborne Raman system can provide daytime water vapor measurements under these conditions that are generally comparable to the measurements provided by the differential absorption LASE instrument. This conclusion is based on the LASE measurement capability demonstrated on August 22, 1998 during CAMEX-3. For nighttime measurements under these conditions, the airborne Raman system offers higher vertical and temporal resolution. For the simulated arctic conditions, measurements in 3 minutes with less than 10% error are possible under nighttime conditions. Under daytime conditions in the arctic using a 10 minute average, the high solar background produces very large errors except near the surface where the random error is approximately 20%. By tuning to a strong absorption line, a differential absorption system such as LASE would likely be capable of improved measurements under these dry daytime arctic conditions.

Also studied was the anticipated performance of an upward looking airborne Raman lidar. These simulations indicated that, from a 10 km flight altitude with a 10 minute average and using 1 km vertical smoothing, profiles with 10% random error are possible up to 14 km.

These results demonstrate that there are significant advantages to operating a Raman lidar looking down from an aircraft versus looking up from the ground. Based on ground-based CART Raman lidar nighttime measurements studied in the first case, the dynamic range of the water vapor signal covered approximately 4 orders of magnitude from the surface up to 8 km. The model simulations indicate that this same water vapor profile when measured from an aircraft would cover

approximately 1 order of magnitude of dynamic range. Significant dynamic range compression exists for the nitrogen signal as well. This means that a single detector channel can be used from an airborne platform to measure either the water vapor or nitrogen profile from near the flight altitude of 10 km to the surface. This can be compared to the two channels that are required to make the same measurement using a ground-based Raman lidar system. Dynamic range compression also implies that shorter averaging times are required to produce good quality signals throughout the profile. Since the concentrations of both water vapor and nitrogen typically increase from 10 km toward the surface, the inverse range squared decrease in the lidar signal intensity is compensated for by the increased concentration of scatterers near the ground. This allows low random error profiles to be acquired in as little as 10 seconds.

The Raman technique has the further advantage that numerous additional measurements can be made with the same system while it is also measuring water vapor mixing ratio. These measurements include aerosol scattering ratio/extinction/depolarization and cloud properties such as liquid water, droplet radius and number density [15]. These measurements are very difficult or impossible with a differential absorption lidar system. For example, aerosol scattering ratio can be calculated directly with a Raman system without resorting to a radiosonde measurement of density or a model atmosphere. Aerosol extinction calculations are also possible with many fewer assumptions using a Raman lidar than with a differential absorption lidar. By including the recently demonstrated capability to retrieve cloud droplet radius and number density using the Raman technique, a measurement not possible with differential absorption lidar, an extremely powerful airborne lidar system is possible.

7 Acknowledgments

This effort has been supported by NASA's Instrument Incubator Program. The authors wish to thank Dave Turner of the Pacific Northwest National Laboratory for access to the raw CART Raman lidar data used in this study. In addition, we thank Rich Ferrare, Ed Browell and Syed Ismail for use of the LASE data.

8 References

[1] Bosenberg, J., 1998: Ground-based differential absorption lidar for water-vapor and temperature profiling: methodology, *App. Opt.*, 37, 3845-3860.

[2] Browell, E. V., 1995: "First Lidar Measurements of Water Vapor and Aerosols from a High-Altitude Aircraft", OSA Optical Remote Sensing of the Atmosphere Technical Digest, Vol. 2, pp 212-214, (1995).

[3] Burris, J., W. Heaps, B. Gary, W. Hoegy, L. Lait, T. McGee, M. Gross, U. Singh, 1998: Lidar temperature measurements during the Topical Ozone Transport Experiment (TOTE)/Vortex Ozone Transport Experiment (VOTE) Mission, *J. Geophy. Res.*, V. 103, D3, 3505-3510.

[4] Evans, K., S.H. Melfi, R. Ferrare, D. Whiteman, 1997:"Upper Tropospheric Temperature Measurements with the use of a Raman Lidar", *Appl. Opt.*, 36, No 12, 2594 - 2602

[5] Ferrare, R. A., S. H. Melfi, D. N. Whiteman, K. D. Evans, R. Leifer, 1998: Raman lidar measurements of aerosol extinction and backscattering 1. Methods and comparisons. *J. Geo. Phys. Res.*, 103, D16, 19663-19672.

[6] Goldsmith, J. E. M., F. H. Blair, S. E. Bisson, D. D. Turner, 1998: Turn-key Raman lidar for profiling atmospheric water vapor, clouds, and aerosols, *Appl. Opt.*, 37, 4979-4990.

[7] Heaps, W. S. and J. Burris, 1996: Airborne Raman Lidar, *Appl. Opt.*, 35, 7128-7135.

[8] Ismail, S. and E. V. Browell, 1989: Airborne and spaceborne lidar measurements of water vapor profiles: a sensitivity analysis., *Appl. Opt.*, 28, 3603-3615.

[9] Measures, R. M., 1984: Laser Remote Sensing Fundamentals and Applications, Wiley-Interscience.

[10] Melfi, S. H., D. Whiteman, R. Ferrare, 1989, "Observation of Atmospheric Fronts using Raman Lidar Moisture Measurements", *J. Appl. Meteor.*, 28, 789

[11] Melfi, S.H., K. Evans, J. Li, D. Whiteman, R. Ferrare, and G. Schwemmer, 1997:"Observation of Raman scattering by cloud droplets in the atmosphere,*Appl. Opt.*, 36, No. 15, 3551-3559.

[12] Stokes, G. M. and S. E. Schwartz, 1994: The Atmospheric Radiation Measurement (ARM) Program: Programmatic background and design of the cloud and radiation testbed., *Bull. Amer. Meteor. Soc.*, 75, 1201-1221

[13] Whiteman, D.N., S.H. Melfi, and R.A. Ferrare, 1992: Raman lidar system for the measurement of water vapor and aerosols in the earth's atmosphere, *Appl. Opt.*, 31, No. 16, 3068-3082.

[14] Whiteman, D. N., 1999: Application of Statistical Methods to the Determination of Slope in Lidar Data, *Appl. Opt.*, 38, 15, 3360-3369.

[15] Whiteman, David. N., Melfi, S. Harvey, 1999:"Cloud liquid water, mean droplet radius and number density measurements using a Raman lidar", *J. Geophys. Res.*, Vol 104 No. D24 December 27, 31411-31419

[16] Whiteman, D. N., K. D. Evans, B. Demoz, D. O'C. Starr, D. Tobin, W. Feltz, G. J. Jedlovec,

S. I. Gutman, G. K. Schwemmer, M. Cadirola, S. H. Melfi, F. J. Schmidlin, 2000: Raman lidar measurements of water vapor and cirrus clouds during the passage of hurricane Bonnie, submitted to *J. Geophys. Res.*

9 Figures

1) Comparison of the overlap function for a 0.6 m F/4 telescope using the ZeMax optical ray trace program and the Raman lidar model for diffrerent telescope focus settings: 1 km, 2 km, 5 km and infinity. The two sets of overlap functions show good qualitative agreement.

2) Comparison of water vapor mixing ratio measurements of the airborne LASE differential absorption lidar and the ground-based SRL. Also shown is a radiosonde launched at 0022 UTC which was approximately 30 minutes before the aircraft overflight. Both the LASE and the SRL profiles use 3 minute averages.

3) Illustration of model tuning for the optical efficiency parameter. On the left is plotted the simulated SRL water vapor signal for a range of optical efficiencies. On the right is plotted the ratio of the model output to the SRL data (smoothed to 400m resolution for easier interpretation). Notice that the curves are separated throughout the profile. The value of 4% gives the best agreement between the data and the model.

4) On the left is shown the result of using a 4% optical efficiency and changing the value of background radiance in units of 10^{-7} W cm^{-2} sr^{-1} μm^{-1}. Here all curves converge in the lowest part of the profile where the background light level has essentially no influence. The ratio of the model to SRL has been smoothed to 400m for easier interpretation. The value of 0.25 x 10^{-7}gives the best agreement between the data and the model.

5) Comparison of actual 1 minute SRL nitrogen channel data and the output of the Raman model. The two curves agree very well up to an altitude of about 13 km where the SRL aerosol channel shows the presence of a cirrus cloud that was not accounted for in the model.

6) Comparison of radiosonde water vapor profile and 1 minute water vapor mixing ratio as predicted by the model. The model used 1 minute averaging and 75m vertical resolution.

7) Comparison of DOE/CART Raman lidar (CARL) high channel water vapor and nitrogen signals and model simulations. CARL uses a narrow field of view detection technique to enhance daytime measurements. The model is able to accurately simulate CARL narrow field performance.

8) Comparison of a 10-minute nighttime water vapor mixing ratio measurement by the DOE CART Raman lidar and model predictions of the CART system for a 1-minute measurement period. The agreement is excellent above 3 km. Below 3 km, the model simulation is influenced by the lidar overlap function and photon count saturation.

9) Comparison of model output and actual CARL measurements during the daytime on September 27, 1997. The solar zenith was 60 degrees.

10) Comparison of daytime water vapor mixing ratio derived from simulated signals generated by the model and the actual CARL measurements made at 1500 UTC on September 27, 1997. Only the high data channels have been simulated so the curves agree well only above 2.5 km.

11) Model water vapor and nitrogen signals for the described airborne Raman lidar at a flight altitude of 10 km. The data have been converted to count rate (Hz). Both water vapor and nitrogen signals show significant dynamic range compression when compared with figure 7.

12) Simulation of the airborne Raman lidar at a flight altitude of 10 km. A 15 second averaging time is used. The profile has been smoothed as follows: 0 - 6 km: 200m, 6 - 8 km: 120m, 8 - 10 km: 40m. The model error is plotted multiplied by 10 for easier viewing. The random error is approximately 5-7% near the surface.

13) Radiances looking downward from 10 km for a range of solar zenith angles and for three surfaces: ocean, grass and fresh snow. The value of radiance required to match the uplooking daytime measurements ($1.5 \times 10^{-2}\ W\ cm^{-2} sr^{-1}\ \mu m^{-1}$) is as large or larger than any downlooking radiance over ocean or grass surfaces.

14) Simulated airborne retrievals from a flight altitude of 10 km for daytime conditions. The background radiance used was for 38 degree solar zenith angle over a grass surface which simulates the measurement conditions at the time of highest sun angle on September 27, 1997 in northern Oklahoma.

15) Simulated measurements of the airborne Raman lidar using the same atmospheric conditions as those shown in figure 2(Andros Island, Bahamas). The averaging time is 10 seconds and the vertical resolution is as follows: 0-4 km : 200 meters, 4-7 km : 120 meters, 7 - 10 km : 40 meters.

16) Simulated airborne Raman lidar measurements from an altitude of 10 km with background radiance equivalent to a 0 degree solar zenith angle over an ocean surface. The averaging time used was 3 minutes and the vertical smoothing is 0-9 km : 200 meters and 40 meters above.

17) Modeled performance of the airborne Raman lidar system for simulated arctic conditions. Nighttime measurement performance using a 3 minute average is shown on the left and daytime performance using a 10 minute average is on the right.

18) Model comparisons of a down-looking airborne Raman lidar using a 0.4 m telescope for the Andros Island case. The nighttime simulation uses a 20 second average while the daytime simulation uses a 3 minute average.

19) Simulation of the water vapor measurement performance of a 0.4 m aperture Raman lidar

system looking upward from a 10 km flight altitude. A 10 minute average has been used along with 1.05 km vertical smoothing.

Modeled Airborne Raman Lidar System Specifications

Telescope	F/9, 0.6 m Cassegrain with 0.15 m secondary
Laser	50 Hz, 300 mj/pulse tripled Nd:YAG, beam expanded to 80 mm
Filter bandwidth	0.3 nm
Filter transmission	0.5
PMT quantum efficiency	0.23
Total water vapor channel efficiency	1.2%
Total nitrogen channel efficiency	0.6%
Data acquisition	Photon counting at 250 Mhz bandwidth